

Simulation of Plume Patterns Associated with Different Atmospheric Temperature Profiles

MOHAMMAD REZA SAHEBNASAGH[†], VAHID ESFAHANIAN[‡], SAEID GITIPOUR^{*},

GOODARZ AHMADI[§] and KHOSRO ASHRAFI

*Department of Environmental Engineering, Faculty of Environment
University of Tehran, Tehran, Iran*

Fax: (98)(21)61113191; Tel: (98)(21)66400884

E-mail: gitipour@ut.ac.ir

Computational fluid dynamics (CFD) has been used to study the effects of wind velocity and temperature profiles on the patterns of the pollutant dispersion by using the Fluent CFD code for three cases of atmospheric stability conditions. The discrete phase model (DPM) along with Reynolds stress turbulence model (RSM) was used to model the dispersion pattern. For neutrally stable atmospheric condition, the velocity, temperature, turbulence kinetic energy (TKE) and dissipation profiles predicted by the model in downwind direction were compared with the results of other investigators to assess the accuracy of the model. It was observed from the simulation results that the pollutant dispersion and turbulence intensity patterns strongly depend on the temperature profile. In addition, the TKE profile was shown to be a good indicator of the mixing zone and the dispersion patterns. These results can be used to assess environment impact of coastal industries which are under various diurnal temperature profiles.

Key Words: Computational fluid dynamics, Temperature profile, Stability condition, Velocity profile, Plume, Dispersion.

INTRODUCTION

Wind velocity and temperature profiles have a significant effect on the dispersion of pollutants from the smoke stacks or vents of the industrial facilities. Such effects will be much more important when these industrial

[†]Department of Environmental Engineering, Faculty of Environment, University of Tehran, Tehran, Iran.

[‡]Department of Mechanical Engineering, Faculty of Engineering, University of Tehran, Tehran, Iran.

[§]Department of Mechanical and Aeronautical Engineering, Clarkson University, Potsdam, NY, 13699 USA.

plants are located in coastal areas. Possibility of high concentration zones occurring downstream of point source discharges, particularly, in vicinity of industrial complexes or nearby urban areas is of concern. These problems need to be considered when new industrial plants or urban areas are being planned, when new emissions are expected. This has particular relevance for the authorization to operate the industrial plant where ambient considerations need to be assessed for human health and ecological reasons. Such an area can be found in southwest of Iran, at the corner of the Persian gulf, the so-called PETZONE area.

Computer models for calculating dispersion of pollutants within the atmosphere have been available for many years and are generally applicable over scales of up to about 50 km from release point^{1,2}. Commercial CFD software, such as Fluent³, offers a method for modeling air flow and pollutant dispersion. Fluent offers the flexibility to represent the complex conditions such as plume dispersion under various temperature and wind velocity profile, ground heat flux and wind flow turbulence. CFD simulation can provide detailed information of the flow fields (*e.g.* dead zones and accelerated flows), turbulence levels and concentration fields downwind of pollutant source.

Ozoe *et al.*⁴ investigated numerically the characteristics of air pollution in the coastal region in the presence of the land and sea breeze. They integrated the two-dimensional primitive equations of momentum and heat to simulate the wind field of the land and sea breeze. They traced the motion of pollution emitted into the land and sea breeze circulation for 3 d. Stable temperature profile, zero synoptic wind velocity and diurnal temperature sine function of land surface are assumed to model the velocity field and pollutant dispersion patterns using 10 km by 100 m grid sizes. Xu *et al.*⁵ studied the directional characteristics of winds and dry deposition of gas pollutants at the coastline. They found that the atmospheric concentrations were higher during onshore than offshore winds throughout the study period for all the measured chemicals. Their study was based on the atmospheric concentration samples and meteorological data of onshore and offshore wind classes during 1994. Luhar and Hurley⁶ applied the air pollution model (TAPM) which is a three-dimensional prognostic Gaussian model to predict meteorological and air pollution fields for environmental impact assessments and the related air pollution studies. Kouchi *et al.*⁷ investigated the effect of thermal internal boundary layer (TIBL) on the ground level concentration (GLC) and the statistical properties of wind turbulence in a thermally stratified wind tunnel. Numerical simulations using a Lagrangian stochastic dispersion model were also conducted and the results were compared with the wind tunnel results and field observations. They assumed Gaussian distribution for *u* and *v* components of velocity within the TIBL region.

Luhar and Sawford⁸ tested several fumigation models involving typical values of entrainment rate and spreading at the interface of the plume and the TIBL. They observed that many existing models that assume uniform and/or instantaneous vertical mixing in the TIBL, give inaccurate results for large entrainment rate and/or small vertical plume spreading at the plume-TIBL interface. They developed an improved analytical fumigation model based on the probability density function (PDF) approach.

Use of advanced numerical methods is a new approach in environmental studies that can be used for realistic simulation of pollutants dispersion. In this study, the pollutants dispersion is simulated under various stability conditions using the CFD Fluent software. In order to enforce the temperature, velocity, turbulence and dissipation rate profiles, the user-defined function facility of software is implemented.

In this study, the dispersion of pollutant emitted in coastal region is analyzed using a commercial computation model. The governing equations for airflow, heat transfer and pollutant dispersion are outlined and the boundary conditions are discussed. The temperature and velocity profiles are simulated and the results are presented in graphical forms. The plume dispersion results are also presented and discussed. It was shown that the turbulence and temperature gradient significantly affect the pollutant transport.

Governing equations

Governing equations which are discretized and numerically integrated in Fluent are given as:

Continuity:

$$\frac{\partial \rho}{\partial t} + \frac{\partial}{\partial x_i}(\rho u_i) = S_m \quad (1)$$

Momentum:

$$\frac{\partial}{\partial t}(\rho u_i) + \frac{\partial}{\partial x_j}(\rho u_i u_j) = -\frac{\partial p}{\partial x_i} + \frac{\partial t_{ij}}{\partial x_j} - \rho \frac{\partial \overline{u'_i u'_j}}{\partial x_j} + \rho g_i + F_i \quad (2)$$

Energy:

$$\frac{\partial}{\partial t}(\rho h) + \frac{\partial}{\partial x_i}(\rho u_i h) = \frac{\partial}{\partial x_i} \left[k_{\text{eff}} \frac{\partial T}{\partial x_i} \right] - \frac{\partial}{\partial x_i} (\sum_j h_j J_j) + \frac{\partial p}{\partial t} + u_i \frac{\partial p}{\partial x_i} + \tau_{ij} \frac{\partial u_i}{\partial x_j} + S_h \quad (3)$$

Dispersion:

$$\frac{\partial}{\partial t}(\rho m_i) + \frac{\partial}{\partial x_i}(\rho u_i m_i) = -\frac{\partial}{\partial x_i}(J_{i,i}) + R_i + S_i \quad (4)$$

In these equations, ρ = density, t = time, x_i = i th direction, u_i = mean velocity component in x_i direction and S_m = mass source term, p = mean

static pressure, t_{ij} = viscous shear stress tensor, ρg_i and F_i are, respectively, the gravity force and other acting force in i th direction, h = enthalpy, T = temperature, h_j = enthalpy of the j 'th component in the fluid defined as:

$$h_j = \int_{T_{ref}}^T c_{p,j} dT \quad (5)$$

where, c_p = specific heat at constant pressure, J_j = diffusion flux of j 'th component, $k_{eff} = (k + k_t)$ = effective conductivity and k_t = turbulence thermal conductivity. S_h = heat source, m_i = mass fraction of the i ' concentration R_i = mass source or sink flux of the i ' component of reaction and S_i = production of i ' component from a discrete phase in the fluid. These equations are general equations used in Fluent but simplified here for an incompressible fluid, in the absence of discrete phase and absence of heat source or sink. These are considered by selecting the relevant options when the model is set up.

The Fluent software solves the Reynolds averaged equations for air flow, pressure, turbulence parameters and energy field³. The Reynolds stress terms are evaluated by the Reynolds stress model (RSM) which is found to be more suitable for air pollutant dispersion¹. The RSM closes the Reynolds-averaged Navier-Stokes equations by solving the transport equations for the Reynolds stress component, together with an equation for the dissipation rate. For plane flows, this means that four additional transport equations are solved. Seven additional transport equations must be solved in three dimensional flows⁴. The Reynolds stress transport equations is given as:

$$\begin{aligned} \frac{\partial}{\partial t} (\overline{\rho u_i u_j}) + \frac{\partial}{\partial x_k} (\overline{\rho u_k u_i u_j}) = & - \frac{\partial}{\partial x_k} \left[\overline{\rho u_i u_j u_k} + p \overline{(\delta_{kj} u_i + \delta_{ik} u_j)} + \frac{\partial}{\partial x_k} \left(\mu \frac{\partial}{\partial x_k} (\overline{u_i u_j}) \right) \right] \\ & \text{local.derivative} \quad C_{ij}=\text{convection} \quad D_{T,ij}=\text{Turbulent.Diffusion} \quad D_{T,ij}=\text{Molecular.Diffusion} \\ \rho \left(\overline{u_i u_k} \frac{\partial u_j}{\partial x_k} + \overline{u_j u_k} \frac{\partial u_i}{\partial x_k} \right) - \rho \beta \left(\overline{g_i u_j \theta} + \overline{g_i u_i \theta} \right) + p \left(\frac{\partial u_i}{\partial x_j} + \frac{\partial u_j}{\partial x_i} \right) - 2\mu \frac{\partial u_i}{\partial x_k} \frac{\partial u_j}{\partial x_k} \\ & P_{ij}=\text{Stress.Production} \quad G_{ij}=\text{Boyanacy.Production} \quad \phi_{ij}=\text{Pressure.Strain} \quad \epsilon_{ij}=\text{Dissipation} \\ 2\rho \Omega_k \left(\overline{u_j u_m} \epsilon_{ikm} + \overline{u_i u_m} \epsilon_{ikm} \right) + S_{user} \\ & F_{ij}=\text{Production.by.System.Rotation} \quad S_{user}=\text{User.Defined.Source.Term} \end{aligned} \quad (6)$$

The terms $D_{T,ij}$, G_{ij} , ϕ_{ij} and ϵ_{ij} need to be modeled to close the equations. Their relation can be find in Fluent user guide⁴.

The semi implicit (SIMPLE) method is used to discretize, the governing equations (*i.e.*, pressure, velocity, temperature, concentration and other variables). Other theoretical aspects and boundary conditions for the model are discussed as:

Boundary conditions

A 2D domain with a length of $L = 5000$ m and a height of $h = 800$ m is considered for performing the numerical simulation. Wind speed of 5 m s^{-1} (at reference height of 10 m above the ground) and a ground roughness length of 0.10 m, representing agricultural land, are used to calculate the profiles of velocity, turbulence kinetic energy (TKE) and turbulence dissipation rate in domain of study. The inlet velocity profile is calculated based on the log expression⁹:

$$u(z) = \frac{u_*}{\kappa} \ln\left(\frac{z + z_0}{z_0}\right) \quad \text{for } z \leq h \quad (7)$$

where $u(z)$ = wind speed at a height of z above the ground, z_0 = roughness length, u_* = friction velocity which is calculated using reference height velocity, h = domain height and κ = von Karman's constant (0.40). The inlet temperature profiles are defined based on the stability conditions of the atmosphere. These profiles are discussed later in this section. The TKE and dissipation rate profiles are considered similar to the profiles used by Riddle *et al.*¹ which have been obtained from atmospheric dispersion modeling system (ADMS). Atmospheric air as inlet fluid to the domain is assumed to be incompressible fluid with variable density.

Study domain surface is discretized with an unstructured mesh, with greater resolution of the nodes close to the ground. Ground ($z = 0$) is specified as a stationary wall with a specified roughness ($z_0 = 0.10$). The lines of $x = -2500$ m and $x = 2500$ m are specified as inlet and outflow boundaries, respectively. Also $z = 800$ m is specified as a plane of symmetry to specify the boundary condition at the height of 800 m. A grid of 21376 cells were used. The size of the grid near the ground was about 8 m by 0.1 m. The generated unstructured grid is shown in Fig. 1.

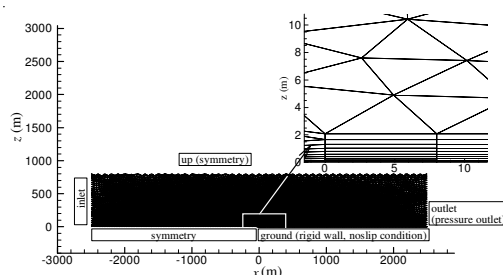


Fig. 1. Generated grid of domain

Fig. 2 shows the inlet profiles of neutral temperature and velocity. Neutrally stable temperature profile considered as adiabatic lapse rate, equal to -0.01 Km^{-1} . The inlet TKE and dissipation rate profiles are shown in Fig. 3. To

check the accuracy of the model, the inlet forced temperature and velocity profiles of neutrally stable atmospheric conditions are compared with the downward locations profiles resulted from simulation. The predicted velocity profiles resulted from running the model show no significant change downstream as shown in Fig. 4a and 4b. These figures compare the velocity profiles throughout the domain with the heights up to 800 and 200 m, respectively. As shown in Fig. 4b main change in velocity profile occurs only near the ground due to wind shear as it is expected¹.

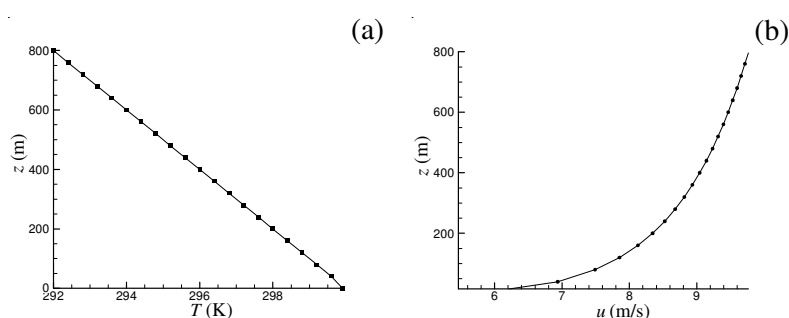


Fig. 2. Inlet profiles (a) temperature and (b) velocity

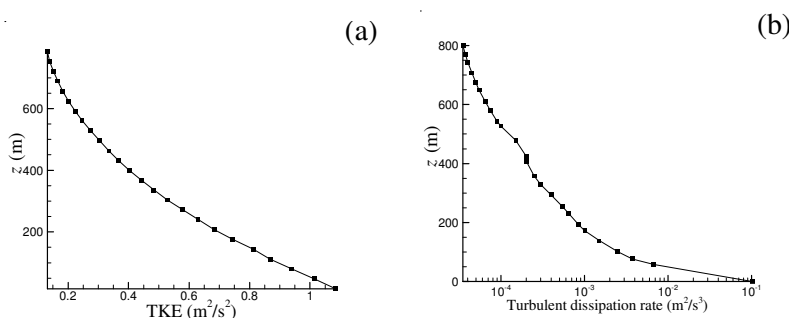


Fig. 3. Inlet profiles (a) TKE and (b) dissipation rate

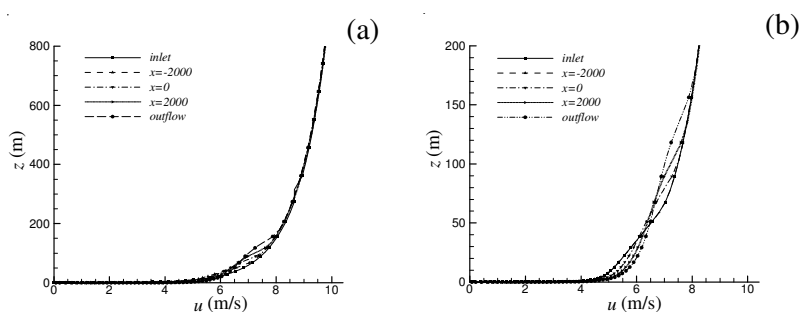


Fig. 4. Velocity profiles comparison throughout the domain, (a) velocity profiles comparison for the height of 800 m (b) velocity profiles comparison for the height of 200 m

The predicted TKE profiles generated by turbulence model at different downward locations of the inlet boundary are shown in Fig. 5. As illustrated in this figure, the TKE level reduces to about 30 % of the inlet value at the ground similar to the results founded by Riddle *et al.*¹. The inlet TKE profile development throughout the downstream is consistent with the atmospheric boundary layer theory. Turbulent effect begins from the end of sublayer. Outside the sublayer up to 10 m, that is called roughness layer, viscous and turbulent effects coexist. Surface layer including sublayer and roughness layer extends to the height of the order of 100 m (turbulent core) from the ground. In the region named as outer layer, above surface layer, turbulence effect reduces to its minimum at free atmosphere^{9,10}. The TKE level increases from zero to its peak value well within the surface layer.

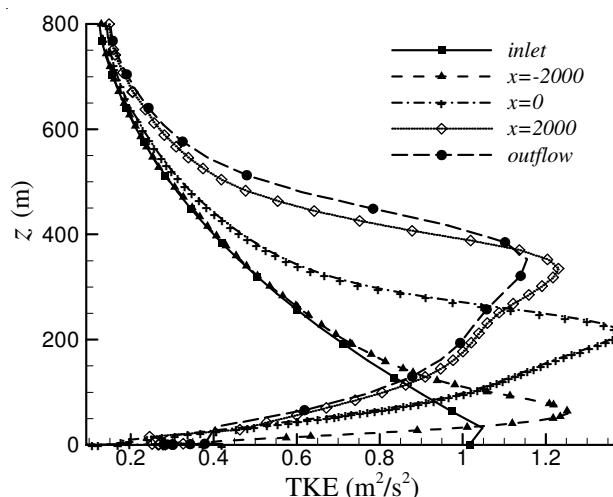


Fig. 5. TKE profiles development from inlet to down winds

Figs. 4 and 5 indicate good agreement of the result of the model with the results obtained by Riddle *et al.*¹. This ensures the accuracy of the model to apply it to predict the pollutant dispersion patterns in the atmosphere.

Fig. 6 shows a similar result for the temperature profiles throughout the domain. As shown in this figure, the simulated profiles are approximately the same as the inlet to the domain.

Stability profiles

Among the main parameters that control the stability conditions of the atmosphere are temperature and velocity profiles. Tables 1 and 2 show the range of parameters corresponding to each class of atmospheric stability condition⁹. Effect of the other parameters such as humidity on dispersion patterns is ignored in this study. Fig. 7 shows temperature profiles of three

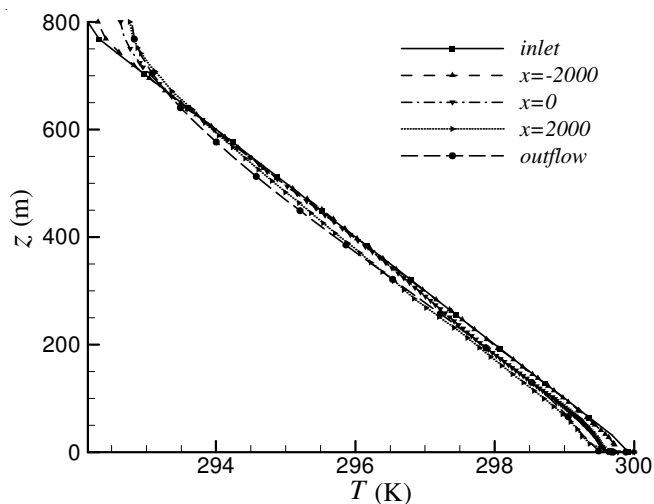


Fig. 6. Temperature profiles throughout the domain

TABLE-1
METEOROLOGICAL PARAMETERS DEFINING
STABILITY CONDITIONS*

Surface (10 m) wind speed (m s ⁻¹)	Day time, Incoming solar radiation			Night time, cloudiness	
	Strong	Moderate	Light	≥ 4/8	≤ 3/8
< 2	A	A-B	B	–	–
2-3	A-B	B	C	E	F
3-5	B	B-C	C	D	E
5-6	C	C-D	D	D	D
> 6	C	D	D	D	D

*A = extremely unstable; B = moderately unstable; C = slightly unstable;
D = neutral; E = slightly stable; F = moderately stable.

TABLE-2
GENERAL CHARACTERIZATIONS OF STATIC STABILITY

Lapse rate	Static stability	$\frac{\partial \theta}{\partial z}$ *	$\frac{\partial T}{\partial z}$ †
Sub adiabatic	Stable	> 0	> - Γ
Adiabatic	Neutral	= 0	= - Γ
Super adiabatic	Unstable	< 0	< - Γ

* $\frac{\partial \theta}{\partial z}$ = Potential temperature gradient, (θ is potential temperature).

† $\frac{\partial T}{\partial z}$ = Temperature gradient and Γ is the adiabatic dry lapse rate.

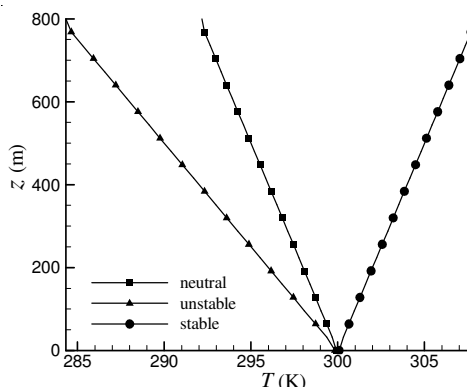


Fig. 7. Temperature profiles corresponding to various stability conditions

(unstable, neutral and stable) classes of atmospheric stability. These three temperature profiles are used to simulate the three stability classes. Moreover, the wind velocity profile generated from equation (5) is considered for all classes of stability.

Plum dispersion set up

The Lagrangian particle (LP) tracking model within Fluent has been used for simulating the gas dispersion. Particles are released from stack and their movement tracked based on the calculated mean wind field and turbulence properties $\overline{u'^2}$, $\overline{w'^2}$ predicted by RSM model. Characteristics of the emission stack released position and the duration of its injection to atmosphere (considered enough large time to ensure the steady state condition) is simulated by Fluent CFD code. Source data are as follows:

- Source location: $x = 0.0$ m, $z = 100$ m
- Source height: 100 m
- Emission particle diameter: 10^{-5} m
- Emission velocity: $v_x = 0.0$ m s⁻¹, $v_z = 20$ m s⁻¹
- Emission flow rate: 0.010 kg s⁻¹
- Temperature: 450 K

Characteristics of generated grid (Fig. 1) and Fluent set up of the model are:

- Unstructured grid of 21376 cells
- Reynolds stress model of turbulence
- Discrete phase model (DPM) of pollutant dispersion

Using RSM model when particle tracking is implemented, turbulence fluctuations for individual coordination directions are used, leading to a non isotropic simulation. It should be noted that the resolution of the particle method is limited by the number of particles tracked. Thus, the method cannot simulate the very low concentrations (*i.e.*, the concentrations below 0.0010 μgm^{-3} in this case).

Grid study made by checking the y^+ (a non-dimensional wall distance) for the first cell. A y^+ value close to the y^+ is most desirable⁴. To fulfill this limitation, y^+ value is adopted using adoption option in Fluent and excessive stretching in the direction normal to the wall is avoided.

RESULTS AND DISCUSSION

Specific conditions of the ambient temperature and wind velocity profiles corresponding to three classes of stability are imposed as inlet boundary conditions to the model. Results of dispersion of pollutant for each case are shown in the Figs. 8-10.

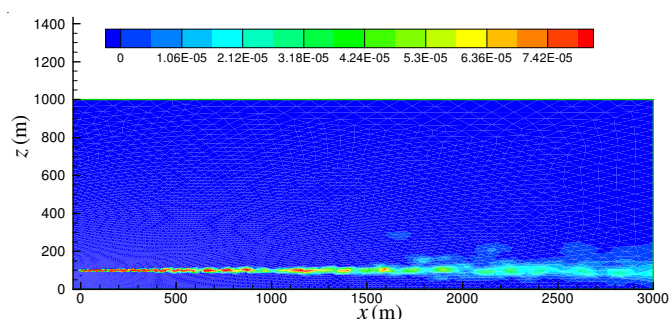


Fig. 8. Concentration pattern for stable condition

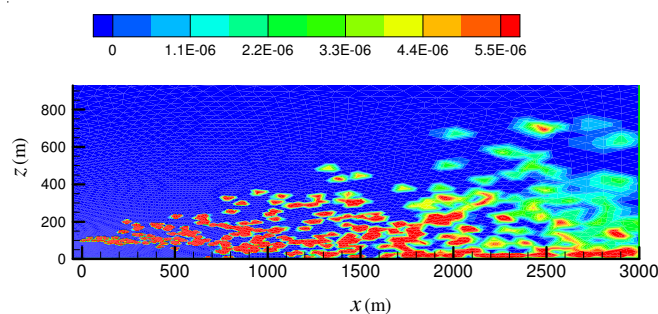


Fig. 9. Concentration pattern for neutral condition

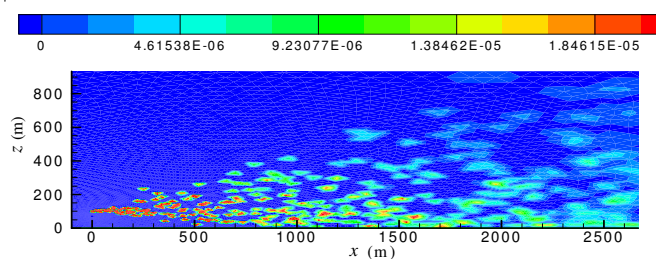


Fig. 10. Concentration pattern for unstable condition

The following results are drawn from the concentration patterns of three stability classes. The pollutant concentrations disperse very quickly to the upper boundary in the neutral and unstable atmospheres, while in the stable atmosphere are still confined at the lower atmosphere as expected. Experimental studies and observations show that stable, neutral and unstable atmospheric conditions cause plumes to develop fanning, coning and looping appearance, respectively. As shown in Figs. 8-10, the same appearance obtained from this numerical study. These figures show that present model takes into account turbulence theories and boundary conditions that specified for it, otherwise considerable errors of implausible concentrations would have been produced at the boundaries. Figs. 11-13 compare the TKE profiles of each stability class in four different distances downwind of the source. From these figures, it is clear that the TKE and its development in z direction for unstable condition is more than neutral and both are more than stable one. Turbulence intensity is an indication of mixing intensity. It is observed that mixing height at $x = 2000$ corresponding to turbulence intensity of $1 \text{ m}^2 \text{ s}^{-2}$ is a wide range from 100 m to about more than 800 m for unstable, but it is from 100-580 m for neutral condition. Turbulence energy of the stable condition is less than $0.250 \text{ m}^2 \text{ s}^{-2}$ in the entire of the domain. Considering the source height of 100 m, the mixing intensity in stable condition corresponds to about $0.260 \text{ m}^2 \text{ s}^{-2}$ of TKE in 500 m downstream of source which reduces to 0.030 for $x = 2000$ m. Plume at this height spreads under TKE intensity of $1 \text{ m}^2 \text{ s}^{-2}$ for neutral condition. Although TKE of $1.40 \text{ m}^2 \text{ s}^{-2}$ is observed at the source height, the maximum TKE level ($2.20 \text{ m}^2 \text{ s}^{-2}$) occurs for unstable condition and this higher intensity over the plume makes it to spread with higher mixing intensity to elevated heights. The TKE intensity for stability classes at $x = 2000$ m are compared in Fig. 14. It is well understood that mixing height of three stability cases at $x = 2000$ m are different (about 400 m with very low TKE for stable and more than 800 m

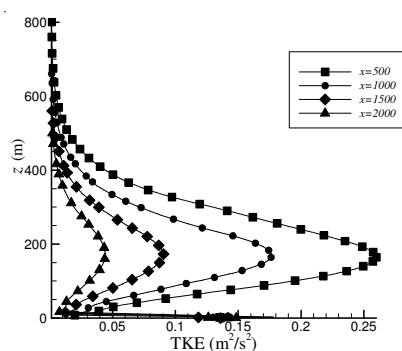


Fig. 11. TKE profile downwind of source for stable condition

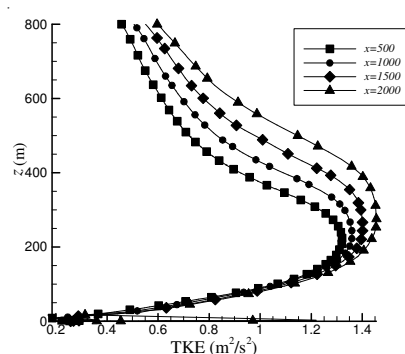


Fig. 12. TKE profile downwind of source for neutral condition

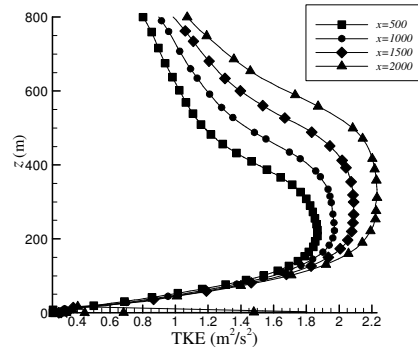


Fig. 13. TKE profile downwind of source for unstable condition

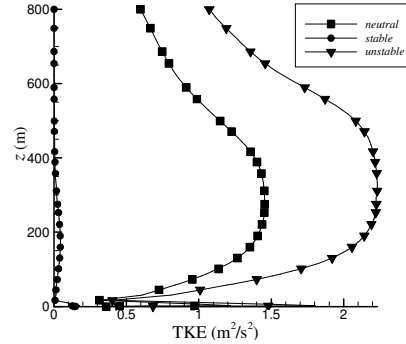


Fig. 14. TKE profile comparison of stability cases at $x = 2000$ m

for neutral and unstable conditions). Fig. 15 shows the Reynolds stress values of $\overline{w'w'}$ and $\overline{u'w'}$ at $x = 2000$ for stable, neutral and unstable conditions. Fig. 16 compares the $\overline{w'w'}$ values for neutral condition at $x = 1000$ and $x = 2000$. These figures show that considerable difference between $\overline{w'w'}$ Reynolds stress values are observed for different stabilities but it is almost uniform downstream of the source for each class.

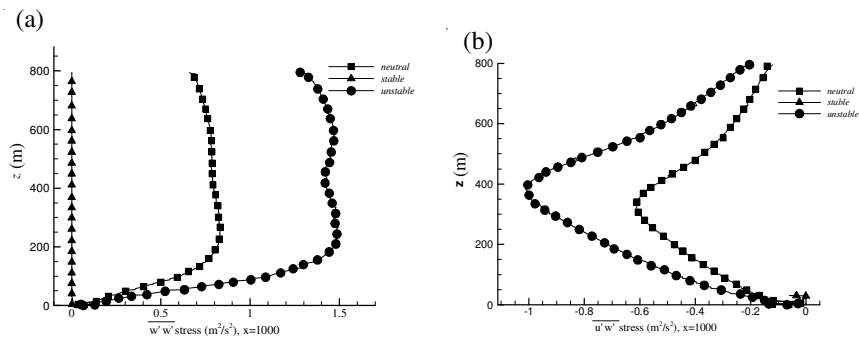


Fig. 15. $\overline{u'w'}$ and $\overline{w'w'}$ Reynolds stress comparison of three classes at $x=1000$

Since the lateral dispersion is ignored in 2D studies, it is reasonable to compare the results with the line source dispersion models. Fig. 17 shows the concentration at source height with Gaussian line source model for neutral case. For this comparison average of 10 snap shuts is used to eliminate the turbulence fluctuation effects. The trends of the both curves are similar and difference is due to dispersion model used in the present study.

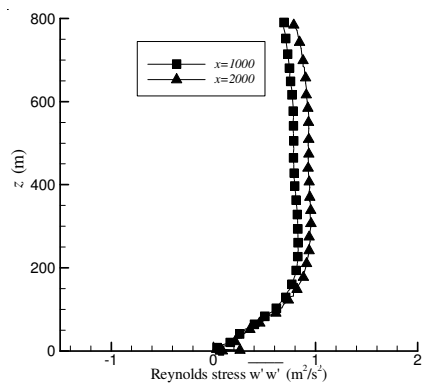


Fig. 16. Stress of neutral condition at $x = 1000, 2000$

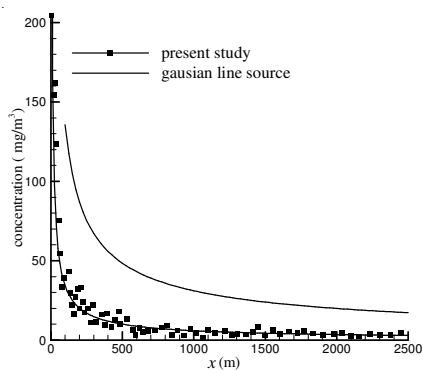


Fig. 17. Concentration of plume at source height, comparison of present study with Gaussian line source formula

Conclusion

Atmospheric temperature and velocity profiles dictate the stability conditions. Significance of atmospheric temperature profile on dispersion of pollutant from a point source is shown in this study. The LP model is based on the stochastic tracking of particles using the individual turbulent fluctuations from the RSM model, thus giving the non-isotropic formulation. The set up of the model for plume dispersion requires consideration of the grid selection of appropriate turbulence and dispersion models. While the forced velocity and the TKE profiles at inlet to the domain are the same for different stability cases, the TKE profiles and Reynolds stress in downwind are significantly different for different cases of temperature profiles given at the inlet. Unstable temperature profile makes higher turbulent kinetic energy particularly in elevated levels. Stable condition damps turbulent energy and plume is dispersed in a limited area around the plume direction with a very low turbulence and subsequently low mixing intensity. This simulation shows that in viscous sublayer, near the ground, small turbulence intensity, particularly for stable condition has small effect on the dispersion of pollutant. The peak turbulence TKE occur where the surface layer ends and outer layer begins. This zone depends on the boundary layer and turbulence parameters which should be considered in environmental air pollution studies.

The set up of the model for plume dispersion requires consideration of the grid generation, appropriate turbulence and dispersion models. The recommended setup conditions determined from this study are listed below:

- Atmospheric air to be considered as a incompressible ideal gas
- Reynolds stress turbulence model
- Velocity, temperature, turbulence model and dissipation profiles specified at the inlet

- y^+ Adaptation is required for better results. It should be more than 30 as suggested by Fluent CFD code.

- It is important to specify correct or realistic boundary conditions for TKE and ϵ at the inlets.

- Using excessive stretching in the direction normal to the wall should be avoided.

- Grid study to be checked by adopting the y^+ value of the cells adjacent to the wall.

Of the most important result, one may consider these parameters in conjunction with dominant temperature and velocity profiles when is going to design the flares, chimneys, vents and stacks. It is well understood that the inversion phenomena which happens due to actual lapse rate gradient change from neutral to stable, leads to lower turbulence intensity. This will retain the pollutant in emitted level in downwind of the source and disperse downward on the ground in case of dense gasses and higher particle diameters which lead to very worst conditions for environment.

ACKNOWLEDGEMENTS

The authors would like to thank the University of Tehran and Bouali-Sina Petrochemical Company for providing research facilities.

REFERENCES

1. A. Riddle, D. Carruthers, A. Sharpe, C. Mchugh and J. Stocker, *J. Atmos. Environ.*, **38**, 1029 (2004).
2. A. Luketa-Hanlin, R.P. Koopman and D.L. Ermak, *J. Hazard. Mater.*, **140**, 540 (2007).
3. Fluent 6.2.16 User's Guide, Fluent Inc. Available from <http://www.fluent.com>. (2002).
4. H. Ozoe, T. Shibata, H. Sayama and H. Ueda, *J. Atmos. Environ.*, **17**, 35 (1983).
5. X. Xu, X. Yang and D.R. Miller, *J. Atmos. Environ.*, **31**, 3729 (1997).
6. A.K. Luhar and P.J. Hurley, *J. Environ. Modeling Software*, **19**, 591 (2004).
7. A. Kouchi, R. Ohba and Y. Shao, *J. Wind Eng. Ind. Aerodyn.*, **81**, 171 (1999).
8. A.K. Luhar and B.L. Sawford, *J. Atmos. Environ.*, **30**, 609 (1996).
9. S.P. Arya, *Air Pollution Meteorology And Dispersion*, Oxford University Press Inc., (1999).
10. K. Muralidhar and G. Biswas, *Advanced Engineering Fluid Mechanics*, Alpha Science International Ltd. Harrow, UK, edn. 2 (2005).

(Received: 16 April 2008;

Accepted: 21 July 2008)

AJC-6718